

## Magnetically Insulated Inertial Fusion: A New Approach to Controlled Thermonuclear Fusion

Akira Hasegawa

*AT&T Bell Laboratories, Murray Hill, New Jersey 07974*

and

Hiroyuki Daido, Masayuki Fujita, Kunioki Mima, Masakatsu Murakami, Sadao Nakai,  
Katsunobu Nishihara, Kiyohisa Terai, and Chiyoe Yamanaka

*Institute of Laser Engineering, Osaka University, Suita Osaka, Japan 565*

(Received 31 May 1985)

By combination of the benefits of magnetic and inertial confinements, a new fusion scheme is introduced with a plasma density of  $\geq 10^{21} \text{ cm}^{-3}$  whose pressure is confined by inertia of a metallic container of a cannonball type while its heat is insulated by a self-generated magnetic field of  $\geq 100 \text{ T}$ .

PACS numbers: 52.75.-d, 28.50.Re, 52.50.Jm, 52.55.Pi

We present a new fusion scheme which can avoid some of the major difficulties faced in the present approaches in magnetic confinement fusion and inertial confinement fusion.

When a plasma with a density of  $\approx 10^{21}/\text{cm}^3$  and a magnetic field of  $\geq 1 \text{ MG}$  is surrounded by a heavy metallic shell, the inertial confinement time can be increased by a factor of  $\approx 10^2$  by the reduction of the sound speed  $u = (T_s/m_s)^{1/2}$ , partly from the larger mass of the shell  $m_s$  and partly from the reduction of the shell temperature  $T_s$  by the thermal insulation due to the magnetic field. This leads to a possibility of achieving ignition of an input energy of  $\approx 1 \text{ MJ}$  without an implosion. Furthermore, since the input energy is directly put into the fuel plasma (rather than the imploding pusher), the present scheme has a better energy efficiency than the inertial fusion scheme. This scheme also eliminates the first wall problem in the magnetic fusion approach.

The basic structure of the plasma container consists of a spherical metallic shell with outer radius  $c$  and inner radius  $b$  in which a solid DT fuel is coated between the radius  $a$  and  $b$  as shown in Fig. 1(a). The gas plasma at  $r < a$  is produced by ablation of the solid fuel caused by an injected laser (or particle) beam through the hole on the top. The laser creates a toroidal magnetic field as a result of the current loop produced by the ejected hot electrons (a  $\nabla n \times \nabla T$  process) which rapidly expands because of the  $E \times B$  drift of electrons throughout the inner portion of the shell as shown in Fig. 1(b). There exists a large amount of experimental evidence<sup>1</sup> of laser-produced magnetic fields beyond  $10^2 \text{ T}$  in an area much larger than the laser spot size. The simulation results obtained by Forslund and Brackbill<sup>2</sup> demonstrate the feasibility of the mechanism assumed in Fig. 1(b). When the inner surface of the solid fuel is heated by

electron depositions and by multiple photorelections, plasma is ejected, carrying the magnetic field from the surface through ablation, and a hot, low-density core is formed in the central region of the shell. If the heat confinement time is made longer than the inertial confinement time by the magnetic field, the ignition condition is given by<sup>3</sup>

$$\frac{r}{4u} (= \tau_{\text{inert}}) > \frac{6T}{E_\alpha} \frac{1}{n \langle \sigma v \rangle}, \quad (1)$$

where  $T$  and  $n$  are the initial plasma temperature and density,  $E_\alpha = 3.5 \text{ MeV}$ , and  $\langle \sigma v \rangle$  is the fusion cross section.

Experiments to check the confinement time have been performed by use of the LEKKO VIII CO<sub>2</sub> laser system<sup>4</sup> of Osaka University which delivers 300 J in 1 ns and spherical targets of C<sub>8</sub>H<sub>7</sub>Cl with 15- $\mu\text{m}$  thickness with diameters ranging from 1 to 3 mm.<sup>5</sup> The energy lifetime of the plasma is measured by the duration of the soft x-ray signals (0.1 ~ 1 keV) emitted from the plasma, the plasma size by x-ray pinhole image, and the temperature by spectroscopic method by use of Na-line intensity ratio. Two types of targets, one having one hole and the other having two holes, were used with a 100-J,  $f = 1.5$  laser per hole focused at the center of the target. The typical x-ray pinhole image and the x-ray signal are shown in Figs. 2(a) and 2(b). The measured plasma temperatures were typically 300 to 400 eV. Figure 3 shows the observed plasma energy lifetime as a function of the cavity diameter when the target is irradiated by a 100-J CO<sub>2</sub> laser. The different lines correspond to the entire width (solid circles), the width of the secondary peak (triangles), and the separation between the two peaks (squares) of the x-ray signals. The first peak is due to the direct impact of the laser, while the second peak is due to the plasma formed in the center. Figure 4 shows the flow

diagram [4(a)] and the profile [4(b)] of plasma pressure,  $p$ , ion density,  $n_i$ , and the electron temperature,  $T_e$ , at 6 ns obtained using a 1D spherical simulation code (HISHO) in which the radial heat conductivity is reduced by  $(\omega_{ce}\tau_e)^{-2}$  starting at  $t=2$  ns with an assumed magnetic field of  $10^3$  T of uniform intensity. A

Gaussian pulse shape is assumed with the peak corresponding to 1.5 ns in the vertical scale in Fig. 4(a). The formation of a hot core with the radius of  $250 \mu\text{m}$ , the electron density  $n (= 3n_i)$  of  $6 \times 10^{20}$ , and the temperature of 600 eV is clearly visible. Both the size of the hot core and the lifetime of the plasma temperature agree very well with the experimental result at 1- and 2-mm diameters. The simulation without the magnetic field produced a plasma with lifetime almost one order magnitude smaller than observed.

Since the magnetic field produced by one beam has only the toroidal component, it does not provide an equilibrium with uniform pressure (which the plasma is believed to choose). For the purpose of creating such an equilibrium, attempts are made to introduce field-aligned currents by use of two laser beams at an angle which hit different portions of the target. They produced a systematically longer lifetime as shown by one example denoted by "2-beam" in Fig. 3. In addition a spheromac-type magnetic geometry<sup>6</sup> is tested by

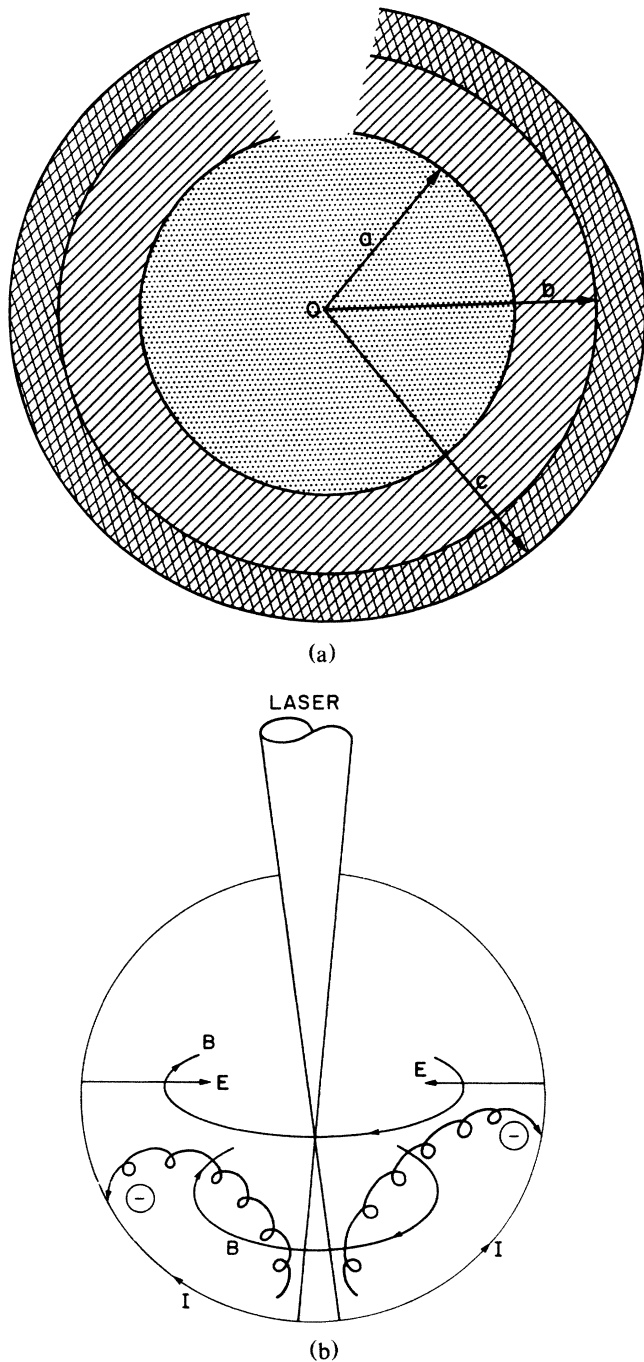
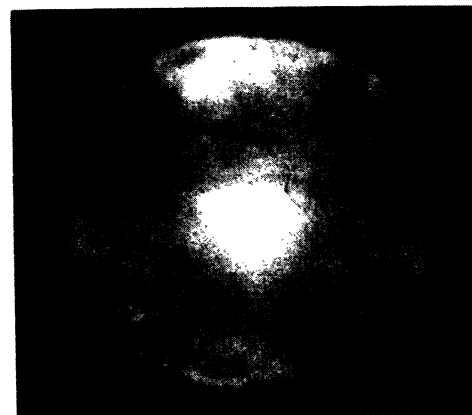
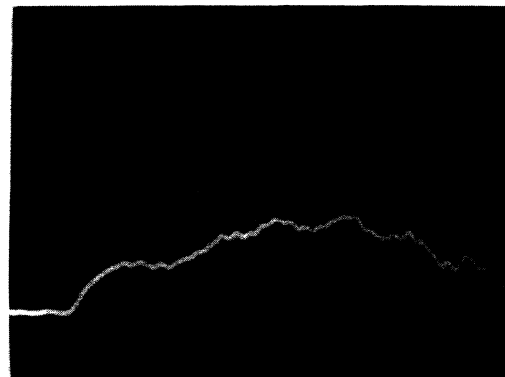


FIG. 1. Schematic diagram of (a) the reactor chamber and (b) process of magnetic field generation.



(a)



(b)

FIG. 2. (a) X-ray pin-hole image and (b) the x-ray signal (0.1 ~ 1 keV) produced in the experiment with a two-hole target with 2 mm diameter by use of two 100-J CO<sub>2</sub> lasers. Sweep time in (b) is 2 ns/div.

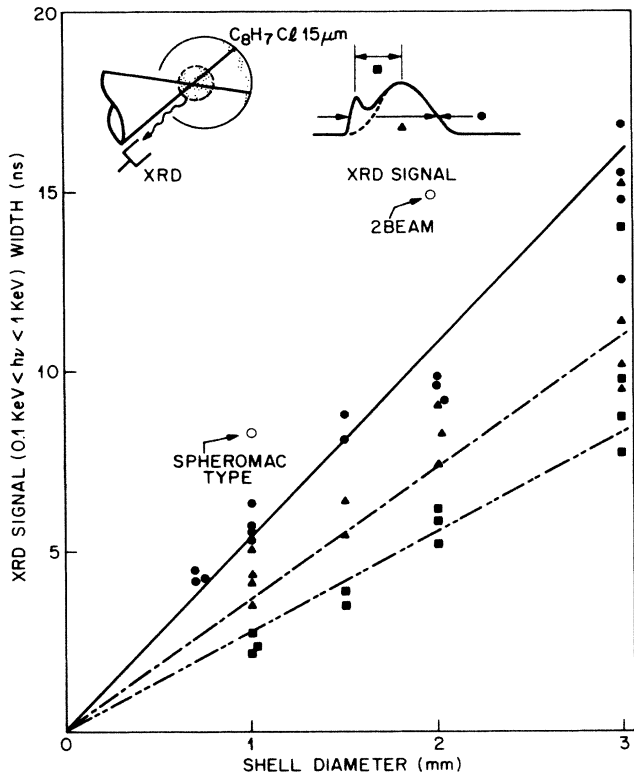


FIG. 3. Observed plasma lifetime as a function of the cavity diameter when the cavity is irradiated by a 100-J CO<sub>2</sub> laser.

use of a one-turn coil which surrounds the sphere azimuthally and by hitting it by another laser with some time advance. The result gave even larger effects as shown by the point indicated by "spheromac type" in Fig. 3. The latter experiment gives further evidence of the existence of the magnetic field. The confinement time of 8 ns observed in the spheromac geometry and the density of  $6 \times 10^{20}$  gives  $n\tau \approx 5 \times 10^{12} \text{ cm}^{-3}$ , which is remarkable as a preliminary set of experiments.

To study the ignition condition, the 1D simulations are extended to the reactor geometry of the type shown in Fig. 1(a) with the fuel (DT) layer of  $300 \mu\text{m}$  and the shell (gold) layer of  $500 \mu\text{m}$ . A magnetic field of  $10^3 \text{ T}$  is applied when the laser power (with the duration of 10 ns) becomes  $10^{-2}$  of its peak value. The observed expansion speeds of the fuel were systematically lower than  $(p/\rho_s)^{1/2}$  by a factor of 1.5 to 2 because of the local heating of the inner surface of the shell, where  $p$  is the plasma pressure and  $\rho_s$  is the mass density of the shell. Because of the reduced speed, the ignitions were observed with the absorbed energies of 0.75 MJ for the shell radius of 2.5 mm.

The target gain is an important factor in the design of the reactor. We find that the gain is a sensitive function of one unknown parameter, the inward dif-

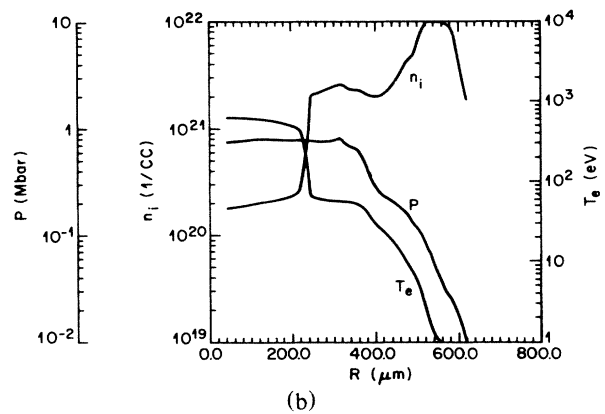
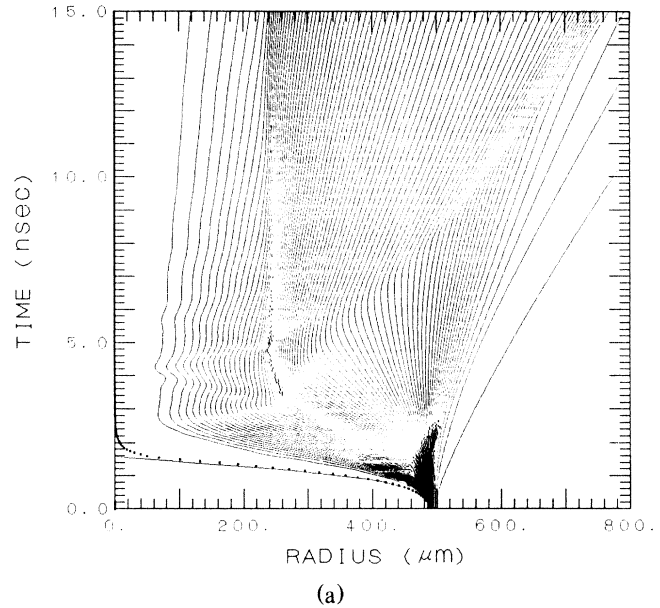


FIG. 4. (a) Flow diagram and (b) the profile of plasma pressure,  $p$ , ion density,  $n_i$ , and the electron temperature,  $T_e$ , at 6 ns based on 1D spherical simulation.

fusion rate of the cold fuel  $u_d$ . The 1D simulations indicate that  $u_d$  is nonzero and close to  $-u$ , resulting in little change in plasma density at the core in the course of expansion. If  $u_d = -u$ , the local plasma internal energy (rather than the volume-integrated energy) increases in time, and detonation occurs if (1) is satisfied. This leads to a large gain ( $\geq 10^3$ ). However, if  $u_d = 0$ , the gain is limited to a relatively small value ( $\approx 30$ ) for a reasonable level of input energy. Thus the proper estimate of the gain factor requires a careful study of the dynamics of the piston front.

The plasma is ideal magnetohydrodynamically stable because of a uniform pressure. The thermal convection would not occur because the effective gravity due to the curvature of the magnetic field is antiparallel to the temperature gradient. The plasma-loss rate from the hole (which may be capped by a clever cavity

design) can be made smaller than the inertial confinement rate if the ratio of the solid angle of the hole to  $4\pi$  is made smaller than the ratio of  $u$  to the plasma sound speed.

One of the authors (A.H.) would like to express his appreciation for critical comments given by Dick Morse and Marshall Rosenbluth.

---

<sup>1</sup>J. A. Stamper, E. A. Mclean, and B. H. Ripin, *Phys. Rev. Lett.* **40**, 1177 (1978); A. Raven, O. Willie, and P. T. Rumsby, *Phys. Rev. Lett.* **41**, 554 (1978); Y. Sakagami, H. Kawakami, S. Nagao, and C. Yamanaka, *Phys. Rev. Lett.* **42**, 838 (1979); M. A. Yates, D. B. van Hulsteyn, H. Rut-

kowski, G. Kyrala, and J. V. Brackbill, *Phys. Rev. Lett.* **49**, 1702 (1982); J. C. Kieffer, H. Pepin, M. Piche, J. P. Matte, T. W. Johnston, P. Lavigne, and F. Martin, *Phys. Rev. Lett.* **50**, 1054 (1983); A. Hauer and R. J. Mason, *Phys. Rev. Lett.* **51**, 549 (1983); K. Terai, H. Daido, M. Fujita, F. Miki, S. Nakai, and C. Yamanaka, *Appl. Phys. Lett.* **46**, 355 (1985).

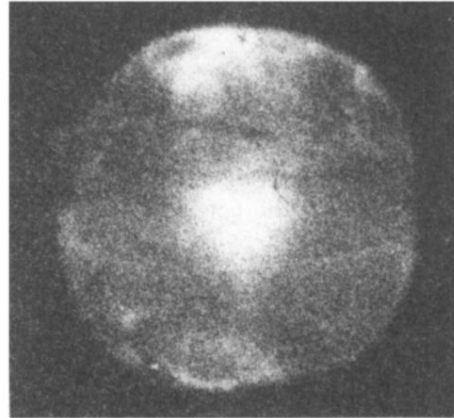
<sup>2</sup>D. W. Forslund and J. V. Brackbill, *Phys. Rev. Lett.* **48**, 1614 (1982).

<sup>3</sup>A. Hasegawa, Reza Kenkyu (to be published).

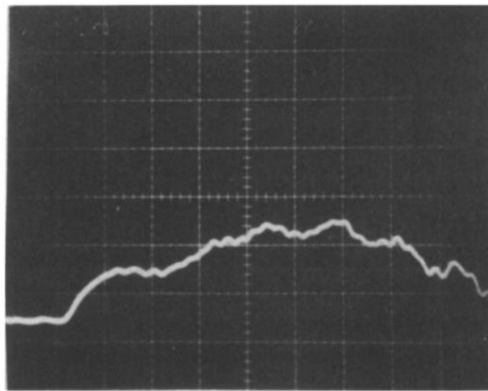
<sup>4</sup>C. Yamanaka, S. Nakai, M. Matoba, H. Fujita, Y. Kawamura, H. Daido, M. Inoue, F. Fukumaru, and K. Terai, *IEEE J. Quantum Electron.* **17**, 1678 (1981).

<sup>5</sup>H. Daido, M. Fujita, K. Tera, F. Miki, K. Nishihara, M. Murakami, K. Mima, S. Nakai, C. Yamanaka, and A. Hasegawa, *Laser Part. Beams* (to be published).

<sup>6</sup>M. N. Rosenbluth and M. N. Bussac, *Nucl. Fusion* **19**, 489 (1979).



(a)



(b)

FIG. 2. (a) X-ray pin-hole image and (b) the x-ray signal (0.1 ~ 1 keV) produced in the experiment with a two-hole target with 2 mm diameter by use of two 100-J CO<sub>2</sub> lasers. Sweep time in (b) is 2 ns/div.

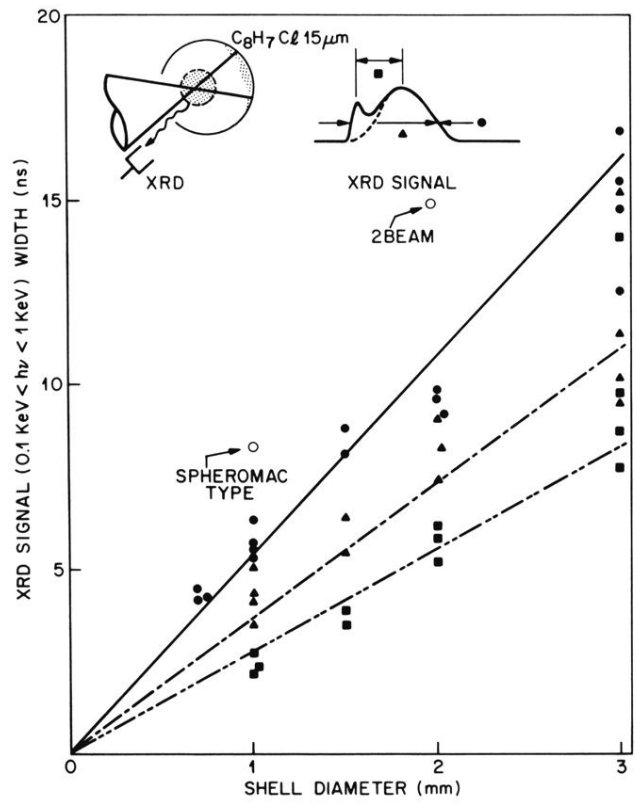


FIG. 3. Observed plasma lifetime as a function of the cavity diameter when the cavity is irradiated by a 100-J CO<sub>2</sub> laser.

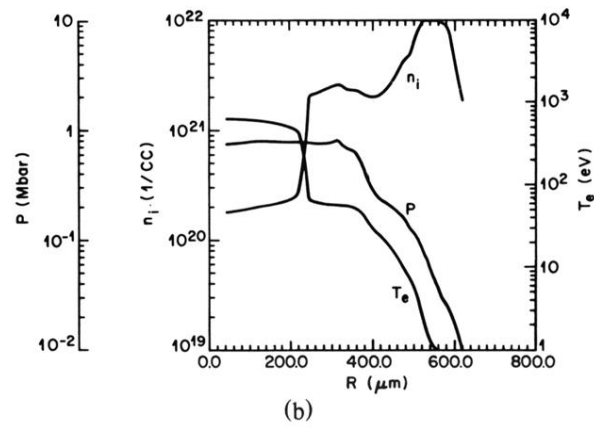
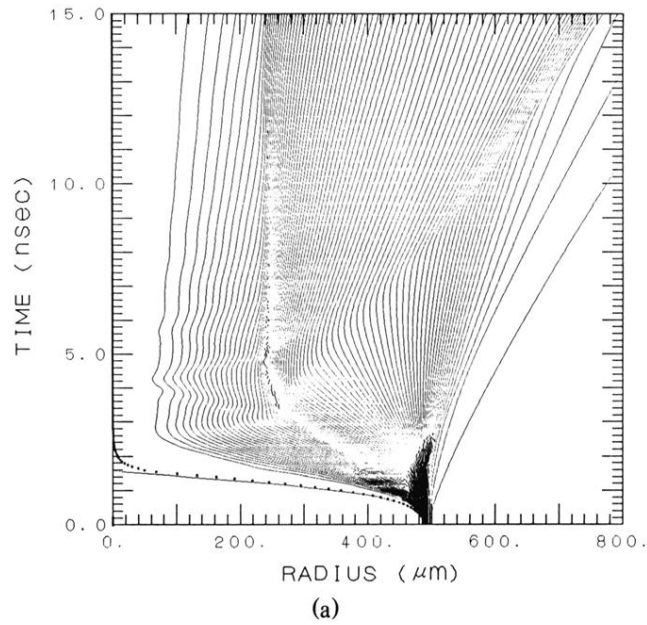


FIG. 4. (a) Flow diagram and (b) the profile of plasma pressure,  $p$ , ion density,  $n_i$ , and the electron temperature,  $T_e$ , at 6 ns based on 1D spherical simulation.